Experimental and Numerical Study of the Heat Transfer Characteristics in Solar Thermal Absorber Tubes with Circumferentially Non-uniform Heat Flux

ARTICLE *in* ENERGY PROCEDIA · JANUARY 2014

DOI: 10.1016/j.egypro.2014.03.033

3 AUTHORS, INCLUDING:

Chun Chang
Chinese Academy of Sciences
24 PUBLICATIONS **352** CITATIONS
SEE PROFILE

Q.Q. Zhang
Institute of Neuroscience
4 PUBLICATIONS **5** CITATIONS
SEE PROFILE

Available online at www.sciencedirect.com

ScienceDirect

Energy Procedia 49 (2014) 305 – 313

Energy Procedia

SolarPACES 2013

Experimental and numerical study of the heat transfer characteristics in solar thermal absorber tubes with circumferentially non-uniform heat flux

C. Chang[a,*], X. Li[a], Q.Q. Zhang[a,b]

[a] *Key Laboratory of Solar Thermal Energy and Photovoltaic System, Institute of Electrical Engineering, Chinese Academy of Sciences, 6 Beiertiao,Zhongguancun,Beijing,100190,China*

[b] *Graduate University of the Chinese Academy of Sciences, Beijing, 1000049, China*

Abstract

This paper presents experimental and numerical studies of the turbulent heat transfer in solar thermal absorber tubes. The absorber tube is a significant component in a solar thermal power system. However, the tube heat transfer performance is different than with other tubes, only half of the circumference surface of the absorber tube is heated with the non-uniform heat flux and the other half is insulated. The non-uniform heat flux on an absorber tube can be up to 1.5MW/㎡ and generates significant temperature difference and thermal stress. The present study uses the experimental and computational fluid dynamics to reveal the turbulent convective heat transfer performance in the solar absorber tube within the range of Reynolds number from1.0×10^4 to 3.5×10^4. The results show that the temperature distribution of fluid and tube wall is very uneven in axial, radial and circumferential direction. The temperature of inner tube wall is an important parameter for preventing the decomposition of heat transfer fluid. The Dittus-Boelter equation is still applicable to calculate the heat transfer in a circular tube with non-uniform heat flux, but it is not suitable to calculate the wall temperature distribution in this condition. The wall temperature distribution of a circular tube with non-uniform heat flux varies with the circular angle of cross section, and this study presents the correlation.

Selection and peer review by the scientific conference committee of SolarPACES 2013 under responsibility of PSE AG.

Final manuscript published as received without editorial corrections.

Keywords: Solar thermal absorber tube; Heat flux; Convective heat transfer; Experimental; Numerical

* Corresponding author. Tel.: +86-10-82671373; fax: +.86-10-62587946

E-mail address: chang21st@mail.iee.ac.cn

Selection and peer review by the scientific conference committee of SolarPACES 2013 under responsibility of PSE AG.

Final manuscript published as received without editorial corrections.

doi:10.1016/j.egypro.2014.03.033

Nomenclature

c_p	Specific heat at constant pressure [$kJ/(kg \cdot K)$]
ρ	Density [kg/m^3]
h	Heat transfer coefficient at tube inner surface [$W/(m^2 \cdot K)$]
A	Surface area of the absorber tube [m^2]
L	Length of the absorber tube [m]
$D_{s,o}$	Diameter of the tube outside [m]
$D_{s,i}$	Hydraulic diameter or diameter of the tube inside [m]
$r_{s,i}$	Radius of the tube inside [m]
$r_{s,o}$	Radius of the tube outside [m]
ν	Kinematic viscosity [m^2/s]
Re	Reynolds number [$UD_{s,i}/\nu$]
λ_f	Thermal conductivity of heat transfer fluid [$W/(m \cdot K)$]
λ_s	Thermal conductivity of tube [$W/(m \cdot K)$]
m	Mass flow rate [kg/s]
Nu	Nusselt number at inside surface [$hD_{s,i}/\lambda_f$]
Pr	Prandtl number [$\rho \nu c_p/\lambda_f$]
T	Temperature [K]
Q	Energy exchanged [W]
q_{max}	The heat flux on tube surface [W/㎡]
u	The radial velocity [m/s]
v	The circumferential velocity [m/s]
w	The axial velocity [m/s]
θ	Circular angle of cross-section [degree]

1. Introduction

Due to the use of thermal storage system and conventional power generation equipment, concentrating solar thermal power (CSP) technology has a smooth and continuous characteristic for electricity supply and has been greatly developed in recent years [1-5]. At the beginning of 2013, about 2.136GW of CSP plants are operating, 2.477GW under construction and 10.135GW are announced mainly in the USA, Spain and China[6]. A CSP plant uses a field of sun-tracking mirrors, to concentrate sunlight onto a solar receiver, where the thermal energy is collected in a heat transfer fluid and then the high temperature fluid is transferred to the steam generator on the ground through pipes to produce high pressure and super-heated steam to a conventional, high efficiency steam turbine to produce electricity [7]. As one of the key component of CSP system, the solar receiver performance affects the operation of the whole power plant. The unsteady and non-uniform radiation flux on the solar receiver surface can be up to 1.5MW/㎡. Absorber tubes are the critically important components in a solar receiver and they absorb concentrated solar radiation to increase the temperature of the working fluid. Many significant experiments and simulations on the receivers of solar power tower system and parabolic trough collector system were published. James and Terry [8] have investigated the thermal performance of cavity receivers of different geometries. They have found that the rim angle and cavity geometry have a strong effects on the energy absorption efficiency. Yu et al. [9] have evaluated and simulated the dynamics performance of solar cavity receiver for full range operation conditions using combined model which mainly couples the radiation–heat conversion process and three heat transfer parameters. They have also tested the effect of wind and DNI on the performance of DAHAN receiver. The

results show that wind angle or velocity can obviously influence the heat losses. Fang et al. [10] have described a methodology for evaluating thermal performance of saturated steam solar cavity receiver under windy environment. To this end, the Monte–Carlo method, the correlations of the flow boiling heat transfer and the calculation of air flow field were coupled to assess absorbed solar energy. They have concluded that the air velocity attained the maximum value when the wind came from the side of the receiver and the heat loss of receiver also reached the highest value due to the side-on wind. Yang et al. [11] have used Computational Fluid Dynamics (CFD) to look into the distributions of temperature, heat flux and the heat transfer characteristics of a molten salt tube receiver. They have concluded that temperature distribution of the tube wall and heat transfer fluid is irregular and the heat flux of the exposed surface rise with the rise of molten salt velocity. Li et al. [12] have performed a steady-state thermal model for 100 kWt molten salt cavity receiver. They have analyzed the effect of optical parameters on the design of such a molten salt receiver. Lu et al. [13] have experimentally investigated the transition and turbulent convective heat transfer performances of molten salt in spirally grooved tube. They have found that the Nusselt number of molten salt flow in spirally grooved tube was higher than that of smooth tube, and the groove height increment can remarkably enhance heat transfer. Zhang et al.[14] have performed experiments to investigate the transient thermal performance (incident power and flow rate) of a 100 kWt molten salt cavity receiver that use electric power as incident radiation. They have obtained that the instantaneous efficiency of the receiver in unsteady state is affected by input power but is not by changes in the flow rate; however, the closer the input power is to the design value, the less the efficiency variation. Zhang et al. [15] have applied the transfer function method (TFM) to estimate the outlet temperature of molten salt cavity receiver and several experiments were conducted to verify the method. The authors obtained a relative error of14.69% sharp variation in the input power accrued. Wu et al. [16] have performed experiments to examine the heat transfer characteristics of molten salt in a circular tube. Found a good agreement between the experimental data of molten salt and numerical correlations. He et al. [17] simulated the energy conversion process in parabolic trough solar collector by a Monte Carlo Ray Trace and Finite Volume Method, the variations of heat flux distributions in different geometric concentration ratios and different rim angles were discussed. Found that with geometric concentration ratios increasing, the heat flux distributions become gentler, the angle span of reducing area become larger and the shadow effect of the absorber tube become weaker. Cheng et al. [18] made the three-dimensional numerical study of heat transfer characteristics in the receiver tube of parabolic trough solar collector and proved that numerical models and methods are feasible.

Since the concentrated solar radiation distribution on the outside wall of the solar absorber tube in parabolic trough collector system (PTC) (Fig.1a) and solar power tower (SPT) receiver (Fig.1b) is very high and circumferentially non-uniform, the failure of thermal stress and thermal distortion of receiver should be evaluated, and the overheating of tube materials and heat transfer fluid materials should be considered to avoid. All these require the accurate calculation of the heat transfer and temperature distribution of the absorber tubes. However, studies on the heat transfer performance and temperature distribution of solar absorber tube with very high and circumferentially non-uniform heat flux are rare. In present paper, experimental measurements and analyses were conducted to investigate the heat transfer performances in a solar thermal absorber tube with circumferentially non-uniform heat flux.

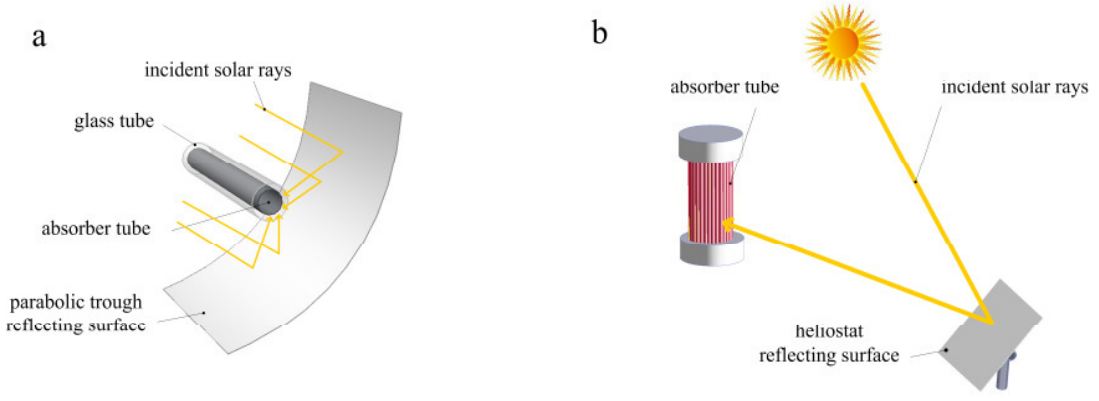

Fig.1 Schematic of an absorber tube (a) parabolic trough collector ;(b)solar power tower

2. Experimental system and numerical model

2.1. General description of the experimental system

The experimental facility mainly included the testing tube, water storage tank, pump, electric power, data acquisition system, flow meter, filter, thermostatic water storage tank, as illustrated in Fig.2. The Volumes of thermostatic water storage tank and water storage tank is 7 m^3 for each. There is a mixing motor installed in the thermostatic water storage tank, which can provide a uniform profile temperature field in the tank. The temperature difference in the tank is less than 0.1℃. Water temperature can be controlled to a desired value in the thermostatic water storage tank by a 20kW electric heater. When the water temperature in the thermostatic water storage tank reaches a prescribed temperature level, pump can be started to circulate water in the cycle.

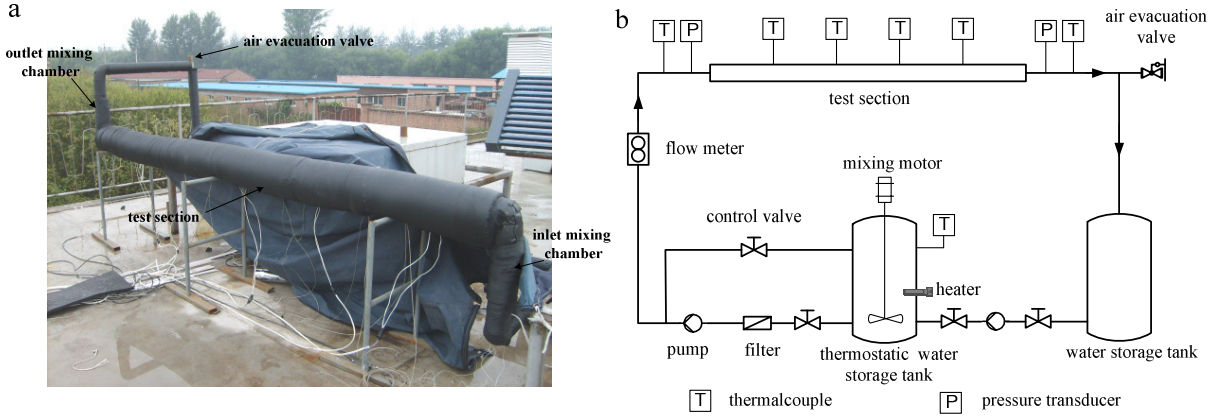

Fig.2 Experimental system (a) experimental installation of test section; (b)Schematic diagram

The test section is a stainless steel absorber tube cooled by water and installed horizontally. The length of the absorber tube L is 3m. The tube inside diameter $D_{s,i}$ is 0.02m and the tube wall thickness is 0.002m.

Fig.3a is the schematic of the test section. The absorber tube is heated by 10 pieces of insulating film electric heaters. The insulating film electric heaters are divided into two groups for topside heating and underside heating. Each of the insulating film electric heaters is 0.6m long and 0.038m wide, and the maximum output power is 1 kW. All the insulating film electric heaters are joined to the tube outside surface by thermal silica and copper shell. When 10 insulating film electric heaters are working at the same power, they can provide circumferentially uniform heat flux to the absorber tube. When only one group topside or underside insulating film electric heaters are working at the same power, they can provide circumferentially non- uniform heat flux to the absorber tube. 32 T type thermocouples located at the positions 0.6m,1.2m,1.8m,2.4m from the inlet, uniformly spaced on each cross section, as showen in Fig.3b. All of the thermalcouples have been calibrated before they were used, and the uncertainty of temperature within 30-350℃ was± 0.3℃.

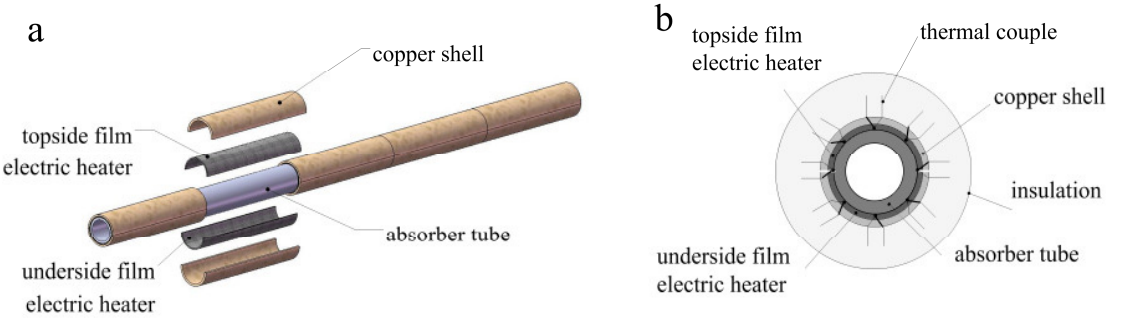

Fig.3 (a) Schematic of the test section; (b) Schematic of the cross section

Two mixing chambers are designed and installed at the inlet and outlet of the test section. The inlet and outlet temperature of the water was measured by Pt100 thermocouples with accuracy of± 0.1℃. The heat flux on the testing tube can be changed to the require value by changing the power of the film electric heaters. The water flow rate is measured by a flow meter with the uncertainty of 0.5%. To obtain the different flow rates, control valves and by-pass channel were used.

2.2. Data analyses

The applied thermal energy of the absorber tube can be described as:

$$Q_f = m_f \cdot c_p \cdot (T_{f,o} - T_{f,i}) \tag{1}$$

At the same time, the heat transfer coefficient h can be calculated from the steady-state energy balance:

$$Q_f = h \cdot A \cdot (T_{s,i} - T_{f,ave}) \tag{2}$$

$$T_{f,ave} = \frac{T_{f,o} + T_{f,i}}{2} \tag{3}$$

$T_{s,i}$ can be obtained from: $$T_{s,i} = T_{s,o} - \frac{Q_f}{2\pi\lambda_s l} \cdot L \cdot \left(\frac{D_{s,o}}{D_{s,i}} \right) \tag{4}$$

The average Nusselt number $\overline{Nu}$ for convective heat transfer in the absorber tube can be calculated as:

$$\overline{Nu} = C\,\mathrm{Re}^m\,\mathrm{Pr}^n \tag{5}$$

The heat transfer coefficient h also behave in the following manner with the Reynolds Re and Prandtl number Pr:

$$h = C \frac{\lambda_f}{D_{s,i}} \mathrm{Re}^m\,\mathrm{Pr}^n \tag{6}$$

Associating all the equations (2), (5) and (6), the average Nusselt number $\overline{Nu}$ can be determined by this equation:

$$\overline{Nu} = \frac{Q_f D_H}{\lambda_f A\left(T_{s,i} - T_{f,ave}\right)} = C\,\mathrm{Re}^m\,\mathrm{Pr}^n \tag{7}$$

Uncertainty analysis is necessary to validate the accuracy of the experimental results. The uncertainties of the calculated results were evaluated using a standard error analysis. The errors of the measured parameters and calculated parameters are presented in Table1.

Table 1. Range of parameters

Item	Range	Inaccuracy
Measured parameters		
Water flow rate	0.173-0.446 kg/s	±0.5%
Water inlet temperature	302.1 K	±0.1 K
Water outlet temperature	303.5 ~ 308.7 K	±0.1 K
Outside wall temperature	304.6 ~ 321.7 K	±0.3K
Calculated parameters		
Heat flux on tube	1926.8-3962.2 W	±0.5%
Nusselt number of water	81.5-199.5	±4.2%

2.3. Numerical model

Fluent6.3 was used and the numerical model involves the prediction of flow and heat transfer behaviors. Some simplifying assumptions are required for applying of the conventional flow equations and energy equations to model the heat transfer process in tube with circumferentially non-uniform heat flux. The major assumptions are:(1)the flow through the absorber tube is turbulent and incompressible; (2)the flow is in steady state;(3)natural convection and thermal radiation are neglected;(4)the thermo-physical properties of the fluid are temperature independent. Based on the above approximations, the governing differential equation is established as flows:

$$\frac{\partial}{\partial t}(\rho\phi)+\nabla\cdot(\rho u\phi)=\nabla\cdot(\Gamma\nabla\phi)+S \tag{8}$$

Where Γ is the diffusion coefficient, and S is the source term. ϕ is a common variable and the quantities Γ and S are specific to a particular meaning of ϕ.

Schematic of uniform heat flux and non-uniform heat flux distribution on the cross section is shown in Fig.4.

The thermal boundary condition of Fig.4a can be established as flows:

$$\lambda\left.\frac{\partial T}{\partial r}\right|_{r=r_{s,o}}=0.5q_{\max},\quad \theta\in[0,2\pi] \tag{9a}$$

$$T(r,\theta,0)=T_0 \tag{9b}$$

$$u(0,\theta,z)=V(0,0,z)=0 \tag{9c}$$

$$w(r,\theta,0)=w_0 \tag{9d}$$

The thermal boundary condition of Fig.4b can be established as flows:

$$\lambda\left.\frac{\partial T}{\partial r}\right|_{r=r_{s,o}}=q_{\max},\quad \theta\in[0.5\pi,1.5\pi] \tag{10a}$$

$$\lambda\left.\frac{\partial T}{\partial r}\right|_{r=r_{s,o}}=0,\ \theta\in(0,0.5\pi)\cup(1.5\pi,2\pi) \tag{10b}$$

$$T(r,\theta,0)=T_0 \tag{10c}$$

$$u(0,\theta,z)=V(0,0,z)=0 \tag{10d}$$

$$w(r,\theta,0)=w_0 \tag{10e}$$

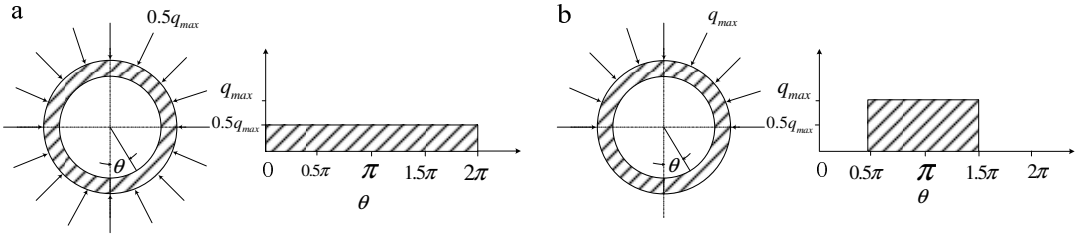

Fig.4 Schematic of thermal boundary condition (a) uniform heat flux;(b) non-uniform heat flux

The grid generation on cross and axial direction is shown in Fig.5 and the temperature and velocity profile on cross section of non-uniform heat flux is shown in Fig.6a and Fig.6b.

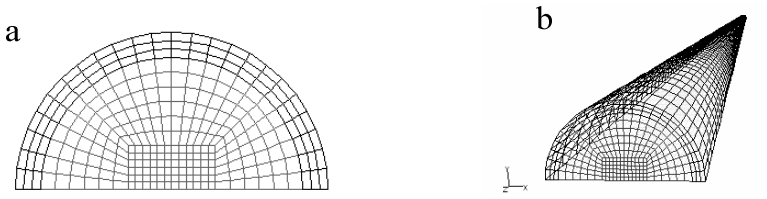

Fig.5 Grid generation(a) on cross section;(b) on axial direction

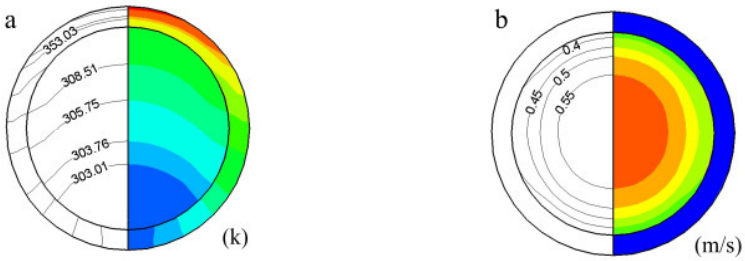

Fig.6 (a)temperature profile; (b)velocity profile on cross section

3. Results and discussion

3.1. With uniform heat fluxes

The experiment on turbulent heat transfer in the absorber tube is to verify the accuracy of experimental facility and numerical model. Reynolds number ranged from 13092 to 32887. The Nusselt number from experimental results, Dittus-Boelter correlation results and CFD simulation results was compared as shown in Fig.7a.

Fig.7a shows the Nusselt number get from experiment tests (Nu-test), coincides well with the Nusselt number obtained from the Dittus-Boelter equation (Nu-DB) , and all data scatter in ±10% of Nu-DB, and so does the Nusselt number obtained from the CFD simulation (Nu-CFD). It is confimed that the accuracy of the experimental test loop and the CFD model is qualified to develop this research.

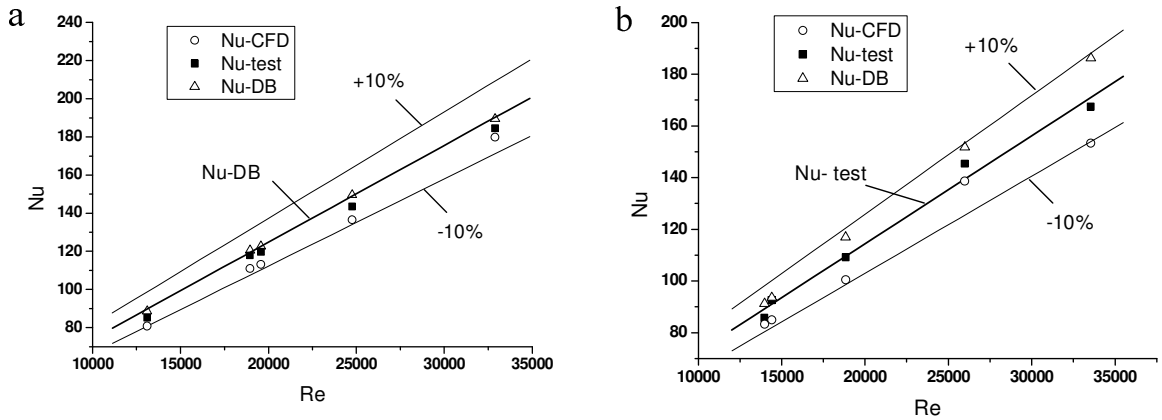

Fig.7 Turbulent heat transfer results of the absorber tube (a) with uniform heat flux;(b) with non-uniform heat flux

3.2. With non-uniform heat fluxes

Fig.7b presents Nusselt numbers obtained from the Dittus-Boelter equation (Nu-DB) were also coincided well with the Nusselt numbers obtained from tests (Nu-test), and all data scatter in ±10% of Nu-test, and so does the Nusselt number obtained from the CFD simulation (Nu-CFD). It confirm that the average turbulent heat transfer coefficient of the circular tube under uniform and non-uniform heat flux can be treated as the same, and Dittus-Boelter equation was still applicable to the calculation of turbulent heat transfer in circular tube with circumferentially non-uniform heat flux.

Fig.8 shows the analysis of tube wall temperature on the cross section which is located 2.4m from the inlet for the non-uniform heat flux case.

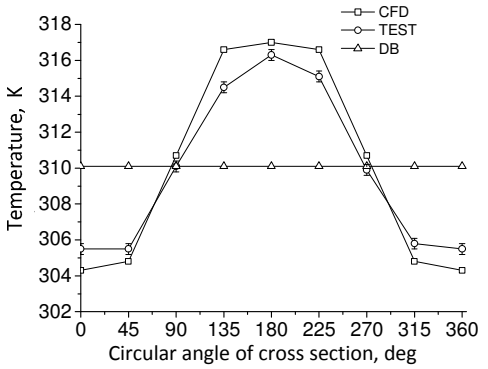

Fig.8 Outside wall temperature distribution on cross section of the test tube with non-uniform heat flux

The outside wall temperature profiles obtained from the Dittus-Boelter correlation is a constant at 310.15 K，but results get from experiment test and CFD simulation are varying with heat flux distribution and the circular angle of cross section.

For turbulent heat transfer in an absorber tube with non-uniform heat flux, the temperature difference between the mean inside wall surface and mean fluid temperature ΔT_i can be calculated using this equation:

$$\Delta T_i = T_{s,i} - T_{f,ave} = \frac{\frac{q_{max}}{2}\frac{D_{s,o}}{D_{s,i}}}{\frac{\lambda_f}{D_{s,i}}Nu} = \frac{q_{max} r_{s,o}}{\lambda_f Nu} \tag{11}$$

The item Nusselt number Nu here can be calculated from the Dittus-Boelter correlation. A series of CFD simulation were made and collated the $T_{s,i}(\theta)$ with $T_{s,i}$, $T_{f,ave}$, and circular angle of cross-section θ. The local temperature of the tube inside surface $T_{s,i}(\theta)$ can be calculated from the regression formula:

$$T_{s,i}(\theta) = T_{s,i} - \Delta T_i \cos\theta = T_{f,ave} + \frac{q_{max} r_{s,o}}{0.023\,\mathrm{Re}^{0.8}\,\mathrm{Pr}^{0.4}\,\lambda_f}(1-\cos\theta) \tag{12}$$

The local temperature of the tube outside wall surface $T_{s,o}(\theta)$ can be calculated from:

$$T_{s,o}(\theta) = \frac{\frac{1}{2} q_{max} r_{s,o} \ln\left(\frac{D_{s,o}}{D_{s,i}}\right)}{\lambda_s}(1-\cos\theta) + T_{f,ave} + \frac{q_{max} r_{s,o}}{0.023\,\mathrm{Re}^{0.8}\,\mathrm{Pr}^{0.4}\,\lambda_f}(1-\cos\theta) \tag{13}$$

4. Conclusion

(1) Comparisons were made between experimental results and the Dittus-Boelter correlation results. Good agreements were found in calculating of the heat transfer in an absorber tube with uniform and non-uniform heat flux. This result indicates that the Dittus-Boelter correlation is still available to calculate the heat transfer in an absorber tube with non-uniform heat flux.

(2) Dittus-Boelter correlation was not suitable to calculate the wall temperature distribution of an absorber tube with non-uniform heat flux. The wall temperature distribution of an absorber tube with circumferentially non-uniform heat flux varies with the circular angle θ of cross-section, and the maximum temperature on the tube wall occurred in $\theta = 180^{o}$.

Acknowledgements

The work is support by National Natural Science Foundation of China (51006096)， Beijing Science and Technology Project（D121100001012001） and National Basic Research Program of China (2010CB227104).

References

[1] Sukhatme SP. Solar thermal power generation. Proceedings of the Indian Academy of Sciences-Chemical Sciences 109(6)（1997）: 521-531.
[2] Tsoutsos T, Gekas V, Marketaki K. Technical and economical evaluation of solar thermal power generation. Renewable Energy 28(6)（2003）: 873-886.
[3] Behar O, Khellaf A, Mohammedi K. A review of studies on central receiver solar thermal power plants. Renewable and Sustainable Energy Reviews 23（2013）: 12-39.
[4] Romero M, Steinfeld A. Concentrating solar thermal power and thermochemical fuels. Energy & Environmental Science 5(11) (2012): 9234-9245.
[5] Price H, Lüpfert E, Kearney D, Zarza E, Cohen G, Gee R, Mahoney R.Advances in parabolic trough solar power technology, Journal of Solar Energy Engineering. 124 (2002) :109-125.
[6] Concentrating solar power: its potential contribution to a sustainable energy future. The European Academies Science Advisory Council (EASAC) policy report 16, November; 2011.
[7] Romero M, Buck R, Pacheco J E. An update on solar central receiver systems, projects and technologies. Journal of Solar Energy Engineering 124(2002):98–108.
[8] JamesA,TerryG.Thermal performance of solar concentrator cavity receiver systems. SolarEnergy1985;34(2):135–42.
[9] Yu Q,Wang ZF,Xu ES.Simulation and analysis of the central cavity receiver's performance of solar thermal power tower plant. Solar Energy 2012;86:164–74.
[10] Fang JB,Wei JJ,Dong XW,Wang YS.Thermal performance simulation of a solar cavity receiver under windy conditions. Solar Energy,2011,85:126–38.
[11] Yang XP,Yang XX,Ding J,ShaoYouyuan et al.,Numerical simulation study on the heat transfer characteristics of the tube receiver of the solar thermal power tower. AppliedEnergy2012;90:142–7.
[12] Li X,Kong WQ,Wang ZF, Chang C,Bai FW.Thermal model and thermo dynamic performance of molten salt cavity receiver.Renewable Energy2010;35:981–8.
[13] Lu J F, Shen X Y, Ding J, Yang JP. Transition and turbulent convective heat transfer of molten salt in spirally grooved tube. Experimental thermal and fluid science, 2013,47:180-185.
[14] Zhang QQ, Li X, Chang C, Wang ZF, Liu H.An experimental study:Thermal performance of molten salt cavity receivers. Applied ThermalEngineering2013;50(1):334–41.
[15] Zhang QQ, Li X, Wang ZF, Chang C, Liu H.Experimental and theoretical analysis of a dynamic test method for molten salt cavity receiver. Renewable Energy2013;50:214–21.
[16]Wu YT, Chen C, Liu B, Ma CF. Investigation on forced convective heat transfer of molten salts in circular tubes. International Communications in Heat and Mass Transfer. 2012,39(10) :1550-1555.
[17] He YL, Xiao J, Cheng ZD,Tao YB. A MCRT and FVM coupled simulation method for energy conversion process in parabolic trough solar collector. Renewable Energy. 2011,36, 976-985.
[18] Cheng ZD, He YL, Xiao J, Tao YB, Xu RJ. Three-dimensional numerical study of heat transfer characteristics in the receiver tube of parabolic trough solar collector. International Communications in Heat and Mass Transfer. 2010, 37, 782-787.